Solar Phys (2008) 250: 279–301
DOI 10.1007/s11207-008-9225-5

Comparison of Solar Magnetic Fields Measured at Different Observatories: Peculiar Strength Ratio Distributions Across the Disk

M.L. Demidov · E.M. Golubeva · H. Balthasar · J. Staude · V.M. Grigoryev

Received: 16 November 2007 / Accepted: 4 June 2008 / Published online: 17 July 2008

Abstract In this paper we analyze the distribution of magnetic strength ratios (MSR) across the solar disk using magnetograms in different spectral lines from the same observatory (Mount Wilson Observatory (MWO) and Sayan Observatory (SO)), magnetograms in the same line from different observatories (MWO, SO, Wilcox Solar Observatory (WSO)), and in different spectral lines from different observatories (the three observatories mentioned above, the National Solar Observatory/Kitt Peak (KP) and Michelson Doppler Imager (MDI) on board Solar and Heliospheric Observatory (SoHO)). We find peculiarities in some combinations of data sets. Besides the expected MSR center-to-limb variations, there is an equator-to-pole asymmetry, especially in the near-limb areas. Therefore, it is generally necessary to use 2D matrices of correction coefficients to reduce one kind of observation into another one.

Keywords Magnetic fields, photosphere · Instrumentation and data management

1. Introduction

The difficulties of a reliable interpretation of solar magnetic field observations are caused by two basic physical problems. Firstly, the object under consideration is complicated itself: the magnetic fields and the thermodynamic parameters of the solar atmosphere show strong inhomogeneities over various spatial scales in the image plane as well as along the line-of-sight. As a consequence, it is rather complicated to model theoretically the various observed

M.L. Demidov · E.M. Golubeva · V.M. Grigoryev
Institute of Solar-Terrestrial Physics, Siberian Branch, Russian Academy of Sciences, 664033 Irkutsk, P.O. Box 291, Russia

M.L. Demidov
e-mail: demidov@iszf.irk.ru

H. Balthasar (✉) · J. Staude
Astrophysikalisches Institut Potsdam (AIP), An der Sternwarte 16, 14482 Potsdam, Germany
e-mail: hbalthasar@aip.de

parameters in the polarized radiation transfer simulations, such as Stokes profile asymmetries in different spectral lines, strength ratios, *etc*. Secondly, there are different instrumental and methodical obstructions for high-precision polarimetric measurements. In this way the interpretation of solar magnetic field measurements with different instruments and/or in different spectral lines becomes a complicated problem. The present paper is mainly devoted to the last mentioned issue in an experimental aspect, *i.e.*, to the comparison of solar magnetic field strengths provided by different data sets.

Indeed, since the beginning of solar magnetographic observations there were vivid discussions and speculations about the relations between registered signals and the real conditions in the solar atmosphere. The question has not yet been solved. A comparison of magnetic field measurements in different spectral lines with the same instrument shows as a rule the discrepancies in measurable values of the strengths and/or other parameters (Howard and Stenflo, 1972; Frazier and Stenflo, 1972; Gopasyuk *et al.*, 1973; Stenflo, 1973; Stenflo, Solanki, and Harvey, 1987; Wiehr, 1978; Semel, 1981; Ulrich, 1992; Shrauner and Scherrer, 1994; Demidov, 2000; Ulrich *et al.*, 2002; Demidov *et al.*, 2002; Demidov, Veretsky, and Peshcherov, 2003; Domínguez Cerdeña, Sánchez Almeida, and Kneer, 2003; Sánchez Almeida, Domínguez Cerdeña, and Kneer, 2003; Socas-Navarro *et al.*, 2008). There are indications that the results depend on the atomic parameters of the compared lines and on the position on the solar disk. Ulrich (1992) even found a dependence on the spatial resolution. The situation becomes even more complicated when a comparison is made using data from different telescopes either for Sun-as-a-star measurements (see the review by Demidov, 2000; as well as more recent results by Demidov *et al.*, 2002; Kotov, Kotov, and Setyev, 2002; Chaplin *et al.*, 2003; Kotov, 2002; Svalgaard, 2005), for active regions (Hofmann *et al.*, 1988; Ronan *et al.*, 1992; Wang *et al.*, 1992; Norton and Ulrich, 2000; Berger and Lites, 2003; Zhang *et al.*, 2003; Su and Zhang, 2007), or for full disk magnetograms (Jones and Ceja, 2001; Arge *et al.*, 2002; Thornton and Jones, 2002; Arge, 2004; Demidov and Golubeva, 2004; Wenzler *et al.*, 2004; Tran *et al.*, 2005).

Such investigations have an important consequence. In particular, the comparison of observations made at the Mount Wilson observatory (MWO) in the lines Fe I λ525.02 nm and Fe I λ523.3 nm (Ulrich, 1992; Ulrich *et al.*, 2002) and at the Wilcox Solar Observatory (WSO) in the lines Fe I λ525.02 nm and Fe I λ524.71 nm (Shrauner and Scherrer, 1994) have been used to estimate the saturation-correction factor for the Fe I λ525.02 nm line measurements and then for the following applications by Wang and Sheeley (1995), Snodgrass, Kress, and Wilson (2000) and Tran *et al.* (2005). Wenzler *et al.* (2004) showed a possibility to construct common long-term data sets from a comparison of magnetograms from National Solar Observatory/Kitt Peak (KP) and the Michelson Doppler Imager (MDI) on board the ESA-NASA satellite Solar and Heliospheric Observatory (SoHO), and to explore the total solar irradiance variations (see also Wenzler, Solanki, and Krivova, 2005). A discussion of the possible dramatic increase of the open magnetic solar flux (Lockwood, Stamper, and Wild, 1999), is made by Arge *et al.* (2002), where data sets of three observatories are involved. The center-to-limb variations (CLV) of magnetic strength ratios $\mathrm{MSR} = B(525.02)/B(524.71)$ as an important parameter for diagnosing the magneto-hydrodynamical structure of the solar atmosphere are used by Solanki *et al.* (1998) and by Demidov, Veretsky, and Peshcherov (2003).

Almost all previous comparisons of solar magnetograms have been restricted to an average value of the scaling factor (mainly relative to the Fe I λ525.02 nm line) with respect to the whole disk (see, *e.g.*, Jones and Ceja, 2001), or by the CLV of this parameter (Howard and Stenflo, 1972; Frazier and Stenflo, 1972; Stenflo, Solanki, and Harvey, 1987; Ulrich, 1992; Ulrich *et al.*, 2002), or by considering it as a function of the distance from the

central meridian (Shrauner and Scherrer, 1994). New investigations of the spatial distribution of MSR over the whole solar disk are necessary. Stenflo and Harvey (1985) have shown that there is a dependence of the strength ratio $B(525.02)/B(524.70)$, and, as a consequence, of the magnetic flux tube properties, on the filling factor and amount of flux, which vary across the disk. Later this result, with the addition of the new thermal line ratio $B(524.70)/B(525.06)$, was confirmed by Zayer *et al.* (1990). The existence of differences between the structures of the plage and network flux tubes was proved by Solanki and Stenflo (1984; 1985). But the only previous study (except a short discussion in Demidov and Golubeva, 2004) with some kind of spatial resolution of the MSR (for the case of MWO and MDI full-disk magnetograms) has been presented by Tran *et al.* (2005), where an analysis was made for ten special zones selected on the solar disk.

Recently, information appeared on the MDI website that this paper by Tran *et al.* (2005) was used as a basic reason for a substantial correction of all MDI magnetic field measurements. On average they must be multiplied by a factor of 1.7. Because our study was started long time before this correction was declared (our paper was already submitted at this time), we used the old, non-corrected SoHO data. This correction, based on the comparison of magnetic field measurements at different instruments, gives additional arguments in favor of the importance of our work.

In the present study we are going on and present a comparison of the Sun's magnetic fields based on full-disk measurements carried out at five observatories, namely, Sayan Observatory (SO), WSO, KP, MWO, and MDI. According to J.W. Harvey's recommendation (2003, private communication), magnetic field strengths from the KP website were multiplied by a factor 1.46. In addition, an investigation of observations at the same observatory, but in different spectral lines, was made where such measurements are available (SO and MWO). Regression and correlation coefficients for different combinations of data sets, covering the whole 2D space across the solar disk, are presented and discussed.

2. Data Sets and Analysis Method

As initial data, 30 full-disk magnetograms with large-scale solar magnetic field (LSMF) measurements, obtained at Sayan Observatory from 1 April to 26 December 2001, have been used. The angular aperture of SO magnetograms is $100''$ and the scanning step is $91''$ in both (EW and NS) directions. This time interval was selected because it was rather close to the maximum of the solar activity cycle (the strength of magnetic fields was rather high), and because the number of Sayan good quality full-disk magnetograms in that year is large enough. For the comparison with other observatories we used the Sayan observations in the Fe I λ525.02 nm spectral line. Basic information of the observations at different observatories is presented in Table 1. The spectral line characteristics are listed in Table 2, where the formation depths are given for the solar disk center.

Ground-based data sets inevitably have gaps due to bad weather or technical problems. However, it is possible to compare 20 pairs of SO – WSO magnetograms, 27 pairs of SO – KP magnetograms, and 26 pairs of SO – MWO magnetograms. Time intervals between comparable observations did not exceed 18 h and were on an average 10.3 ($\pm$0.36) h. The preliminary analysis showed that the solar rotation, taken into account to compensate the differences in time of the recording of comparable measurements, strongly affects the results. Therefore, in all of these cases a solar rotation compensation has been performed according to the law of Howard and Harvey (1970). At that time, the photospheric magnetic field in the corresponding calculations was assumed to be radial. At MDI on board SoHO, solar

Table 1 Observatories and instruments.

Observatory (λ, φ)	Instrument	Spectral line [nm]	Pixel size [arcsec]	Image size [pixels]
SO (100.8°E, 51.6°N)	Solar Telescope for Operative Prediction (STOP). Spectropolarimeter	Fe I λ525.02	91 × 91	21 × 21
WSO (122°W, 37.4°N)	Babcock-Type Solar Magnetograph	Fe I λ525.02	90 × 180	21 × 11
MWO (118.1°W, 34.3°N)	150-Foot Solar Tower Telescope. Multi-Chanel Magnetograph	Fe I λ525.02 Na I λ589.59	3.7 × 3.7	512 × 512
KP (111.6°W, 32.0°N)	Vacuum Telesc. with Spectro-magnetograph	Fe I λ868.86	1.14 × 1.14	1788 × 1788
SoHO	Michelson Doppler Imager (MDI)	Ni I λ676.78	1.98 × 1.98	1024 × 1024

Table 2 Parameters of spectral lines used in comparison between observatories.

Spectral line [nm]	EP [eV]	Landé factor	W_λ [mÅ]	Formation depth [km]	Reference
Fe I λ525.02	0.121	3.00	62	440 (core)	Sheminova (1998)
				260 – 312	Bruls, Lites, and Murphy (1991)
Na I λ589.59	0.00	1.33	564	500 – 790	Ulrich *et al.* (2002)
Ni I λ676.78	1.83	1.43	83	350 (core) 280 (wings)	Vernazza, Avrett, and Loeser (1981)
Fe I λ868.86	2.18	1.66	268	525 (core) 150 (wings)	J.W. Harvey, private communication
				432 – 475	Bruls, Lites, and Murphy (1991)

magnetic fields are registered regularly with a 96-min interval. Each of the basic SO magnetograms was compared with the corresponding quasi-simultaneous MDI magnetogram. In that case the solar rotation compensation was not carried out.

For quantitative comparison of magnetic field measurements in different spectral lines or observatories, methods appropriate for individual cases must be adopted. To avoid the possible influence of zero level problems on the results, Howard and Stenflo (1972) calculated the mean absolute magnetic flux in circular zones at different distances from the disk center. To simplify the comparison of data sets obtained with different spatial resolution,

Table 3 Results of correlation and regression analyses of solar magnetic field measurements in different observatories. $A(\pm\Delta A)$, $R(\pm\Delta R)$ – parameters of the linear regression equation $B_{\mathrm{DataSetY}} = A(\pm\Delta A) + R(\pm\Delta R) \times B_{\mathrm{DataSetX}}$, ρ – correlation coefficient.

Data set X	Data set Y	N	A	ΔA	R	ΔR	ρ
SO	WSO	3900	−0.03	0.08	0.75	0.01	0.85
	KP	9423	0.01	0.28	3.71	0.02	0.82
	MWO (525.02)	9018	0.03	0.09	1.17	0.01	0.84
	MWO (589.59)	9018	−0.35	0.20	2.53	0.01	0.83
	SoHO	10470	0.26	0.20	2.75	0.02	0.83

the histogram-equating method was used by Jones and Ceja (2001), Thornton and Jones (2002), and Wenzler *et al.* (2004). At last, a direct pixel-by-pixel comparison method is used by Stenflo (1973), Ulrich (1992), Ulrich *et al.* (2002), Demidov, Veretsky, and Peshcherov (2003), and Tran *et al.* (2005). This method allows us to study the spatial distribution of strength ratios across the solar disk. It is an urgent task, which has not yet been investigated in an appropriate manner.

In our case in each pair of comparable observatories, the data were reduced to equal spatial resolution, and the lowest one was used. Thus, in order to compare SO – WSO observations, SO magnetograms were interpolated using a standard minimum-curvature spline fit onto the corresponding WSO coordinate grid (21 × 11 matrix, 195 points on the solar disk). To compare SO measurements with KP, MWO, and SoHO/MDI magnetograms, the latter were averaged over the SO aperture (21 × 21 matrix, 349 points on the disk).

3. Results

3.1. Comparison of SO Magnetograms with those of WSO, KP, MWO, and MDI

As the first step, a general statistical analysis of all data sets has been made. The corresponding correlation coefficients ρ and the linear regression parameters were calculated and the results are presented in the corresponding scatter-plot diagrams in Figure 1 and in Table 3. In all five combinations of data (for the MWO observations two spectral lines are used), the correlation coefficients are almost the same and rather high (the highest ρ is 0.85 for the SO – WSO case, and the lowest one is 0.82 for the SO – KP case). But the regression coefficients R (determined by the reduced major axis method, Davis, 1986) differ very significantly from case to case. Comparing SO – WSO and SO – MWO (Fe I λ525.02 nm) observations, performed in the same spectral line, a quite good correspondence is found – the regression coefficients are 0.75 and 1.17, respectively. Concerning SO – KP, SO – MWO (Na I λ589.59 nm), and SO – MDI, when measurements were made in different spectral lines, there are significant systematic discrepancies (the regression coefficients are 3.71, 2.53, and 2.75, respectively).

As already mentioned before, there are many reasons which can cause the differences of magnetic field strengths measured at different observatories in the same spectral lines (different spatial resolution, various instrumental effects, calibration, *etc.*). The situation becomes even more complicated when different spectral lines are used. Nevertheless, we obtain a rather good agreement for three independent data sets, where the line Fe I λ525.02 nm is

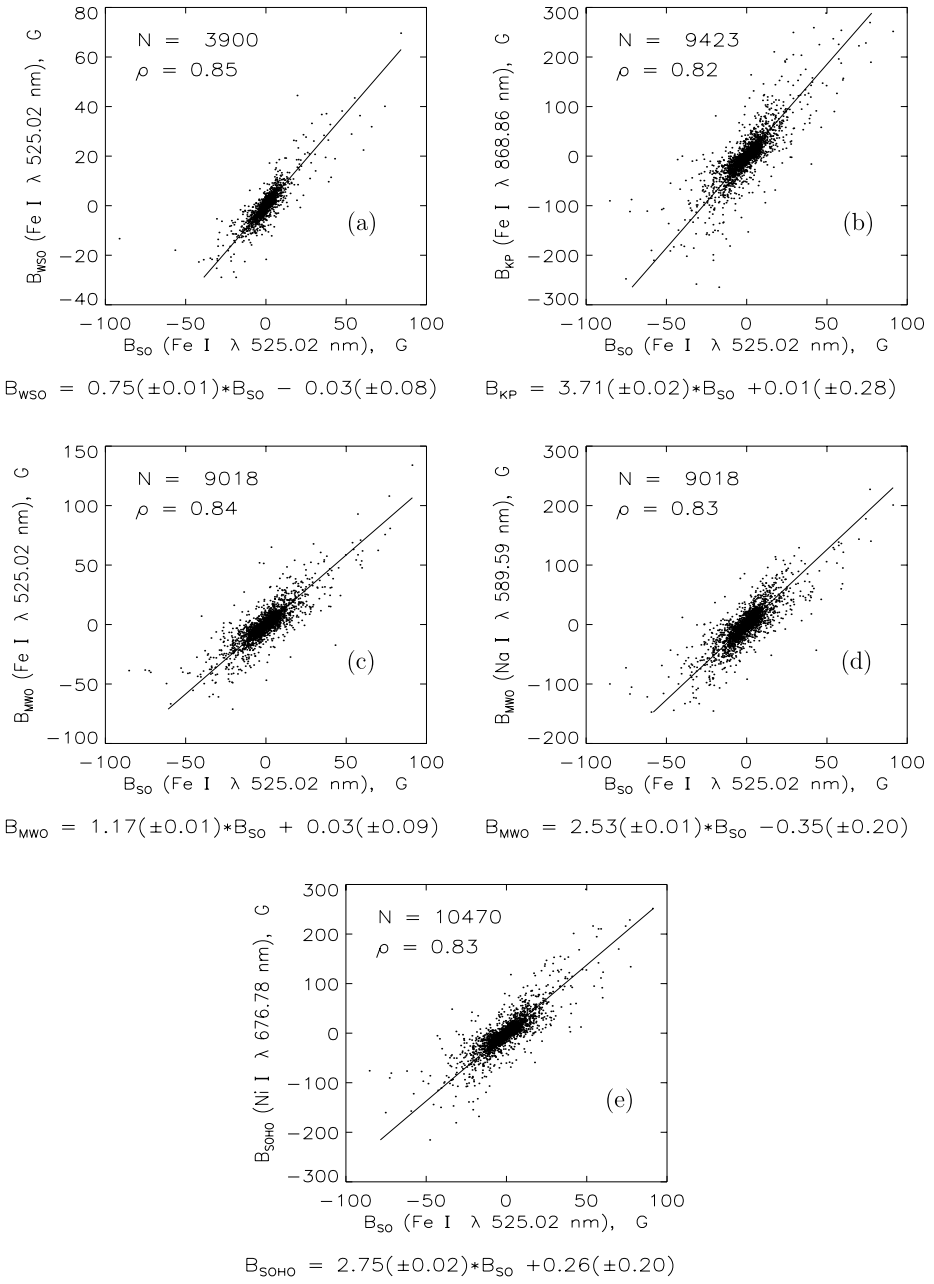

Figure 1 Correlation and regression analysis for different combinations of data sets (a) SO – WSO, (b) SO – KP, (c) SO – MWO (Fe I λ525.02 nm), (d) SO – MWO (Na I λ589.59 nm), (e) SO – MDI. The number of magnetogram pairs are 20, 27, 26, 26, and 30, respectively, N is the number of common points, ρ the correlation coefficient. The linear regression equations are shown at the bottom of each scatter plot.

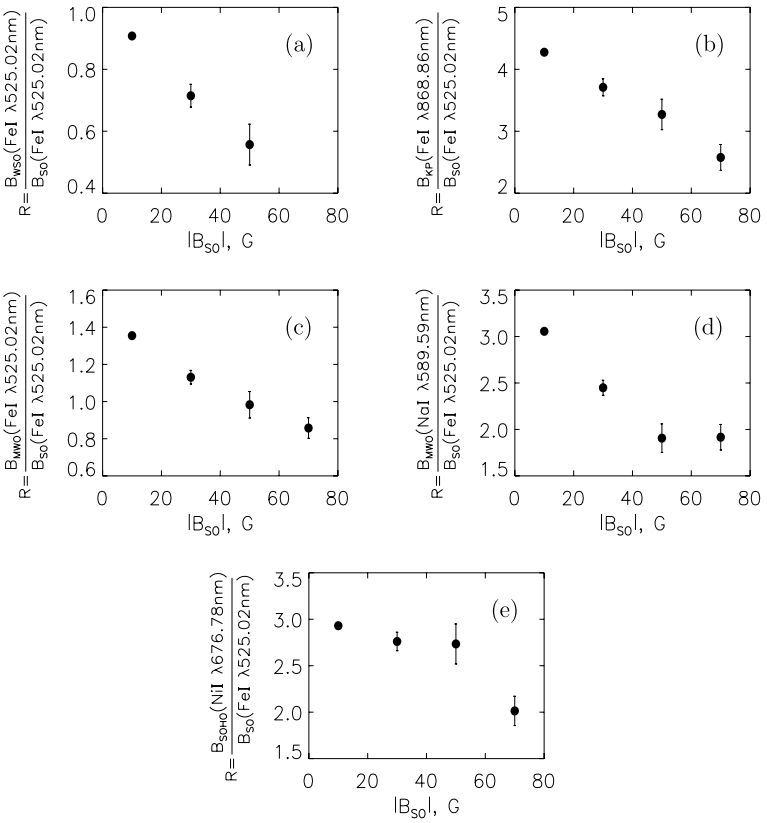

Figure 2 Dependence of the line ratios, considered in Figure 1, on SO magnetic field strength.

used. The fact that WSO shows strengths about 25% lower than SO, and MWO about 17% higher, can be explained by the Schwarz inequality (see Berger and Lites, 2003). Indeed, averaging the high spatial resolution MWO observations down to that of SO, we find stronger values than at SO, and when we degrade SO data to the lower spatial resolution of WSO, we obtain larger strengths at SO than at WSO.

From a careful consideration of the scatter plots in Figure 1 we see differences in the behavior of points of low and high magnetic strength values. The same fact was mentioned earlier by Jones and Ceja (2001). In order to explore this effect in more detail, special calculations of regression coefficients R for different bins of strength B for all combinations of data sets were made. The results are shown in Figure 2, for absolute values of magnetic flux on the x-axis. In all cases we see a decrease, sometimes rather significant, of R with increasing $|B|$. Note that the first bin contains the overwhelming number of points in all cases. For the KP – SO combination there are 9204 points in first bin, 176 points in the second, 32 points in the third, and only 9 points in the fourth. Therefore, the average value of R is clearly dominated by the first two bins. The reason for this nonlinearity of R is not clear, but it can have important consequences.

Our aim is not restricted to the determination of average correction factors between different data sets. Of special interest is the question: how such factors are spatially distributed across the solar disk? Therefore, a more sophisticated study has been done. For each pair

of comparable data sets the 2D matrices (with dimensions, as mentioned above, determined by the observations with the lowest spatial resolution) have been computed. To do that for each individual element ("pixel") of the matrices we constructed pairs of time series of magnetic field strengths, observed by the compared observatories in the corresponding solar disk point. Then the parameters of the linear regression equations and the correlation coefficients for each matrix element were calculated.

The distributions of the regression R and correlation coefficients ρ are plotted in Figure 3 in mosaic form. These distributions allow to estimate the reliability of the regression coefficients in different parts of the solar disk. We conclude that the center-to-limb variations of the regression coefficients R can be seen in all cases. These variations are rather small for the SO – WSO and SO – MWO (Fe I λ525.02 nm) combinations, although there are some peculiarities in the polar regions. The CLVs of the regression coefficients for the SO – KP, SO – MWO (Na I λ589.59 nm), and SO – MDI data are very large. There are big discrepancies between the R values in the equatorial and in the near-polar regions for the SO – KP case. In the SO – MDI case there is a pronounced asymmetry between E and W hemispheres. This E – W asymmetry was found by Tran *et al.* (2005) as well as in the comparison between MDI and MWO data.

It is well known that magnetic flux is inhomogeneously distributed across the solar disk. In combination with the aforementioned dependence of line ratios on the magnetic field strength, it is quite natural to suppose the existence of links between spatial distributions of R and $|B|$. To explore such a possibility, the distributions of the absolute values (modules) of $|B|$ across the solar disk for all data sets were calculated. In all six cases they look very similar. The examples for two cases, SO and KP, between which the differences are most significant, are shown in Figure 4. As it was expected, the magnetic flux is concentrated in two belts near the equator plane. At the equator itself and at the polar zones, the concentration of flux is drastically weaker. From the detailed comparison with mosaics at Figure 3, it is easy to see serious differences in spatial structures of R and $|B|$: the R mosaics are more symmetrical and there is no equatorial gap. This simple consideration shows that the spatial distribution of $|B|$ is not responsible for the peculiarities of the spatial distributions of R.

A special analysis was carried out to explore possible differences in the CLVs of R in the equatorial and the polar directions of the solar disk. First, the solar disk was divided into circular zones of width $\Delta\mu = 0.1$, where $\mu = \cos\theta$, and θ is the heliocentric angle. Then four 90° sectors (polar sectors N and S, equatorial sectors E and W), beginning from the disk center, were selected and for every arch of each sector the corresponding R coefficients were calculated. Finally, to improve the statistics, the results for two polar and two equatorial sectors were averaged into combined NS and EW sectors, respectively. The results for all combinations of data sets are presented in Figure 5. The increase of the mean errors of values towards the limb is caused by the decreasing number of points involved in the processing (for the $0.1 < \mu < 0.2$ range there are only four points in the extreme case).

In the SO – WSO and SO – MWO (Fe I λ525.02 nm) cases, when data sets are obtained in the same spectral line, CLVs of regression coefficients R are rather small at heliocentric angles within 60° ($\mu \geq 0.5$) and almost indistinguishable in N – S and E – W sectors, whereas some discrepancies are observed near the limb. The comparison of SO – MWO (Na I λ589.59 nm) and SO – KP magnetograms brings out the discrepancies in CLVs of the R coefficients in E – W and N – S sectors, beginning with small heliocentric distances. In the case of SO – KP, near-limb values of R are two times larger near the equator than at the poles. The analysis of SO and MDI data does not show a significant polar – equator asymmetry in the R coefficient distribution. However, in this case a considerable decrease of R by a factor of three is observed when passing from disk center to limb.

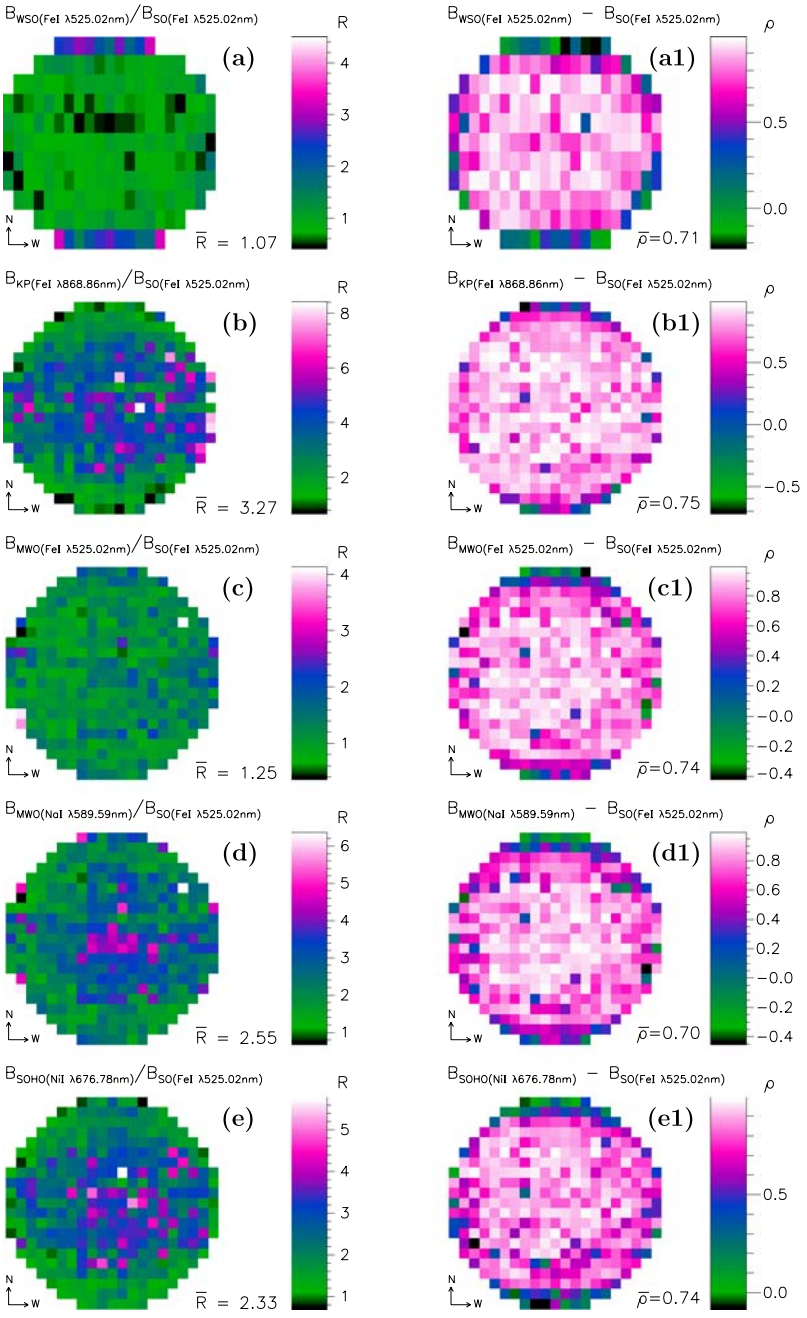

Figure 3 2D distributions of regression (left panels, (a) – (e)) and correlation (right panels, (a1) – (e1)) coefficients across the solar disk, together with the corresponding color scale bars, for the different combinations of data sets: (a) WSO – SO, (b) KP – SO, (c) MWO – SO (Fe I λ525.02 nm), (d) MWO – SO (Na I λ589.59 nm), (e) MDI – SO. For each case, the number of used magnetograms is the same as in Figure 1.

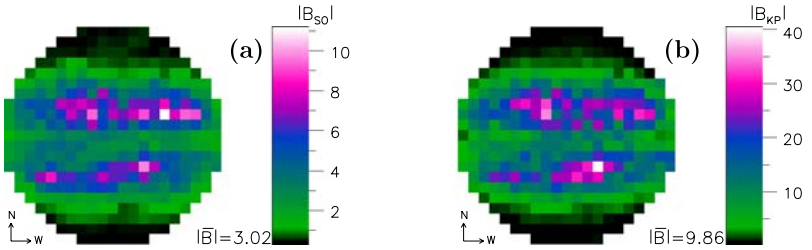

Figure 4 2D distributions of absolute magnetic flux $|B|$ across the solar disk for SO (a) and KP (b) observatories.

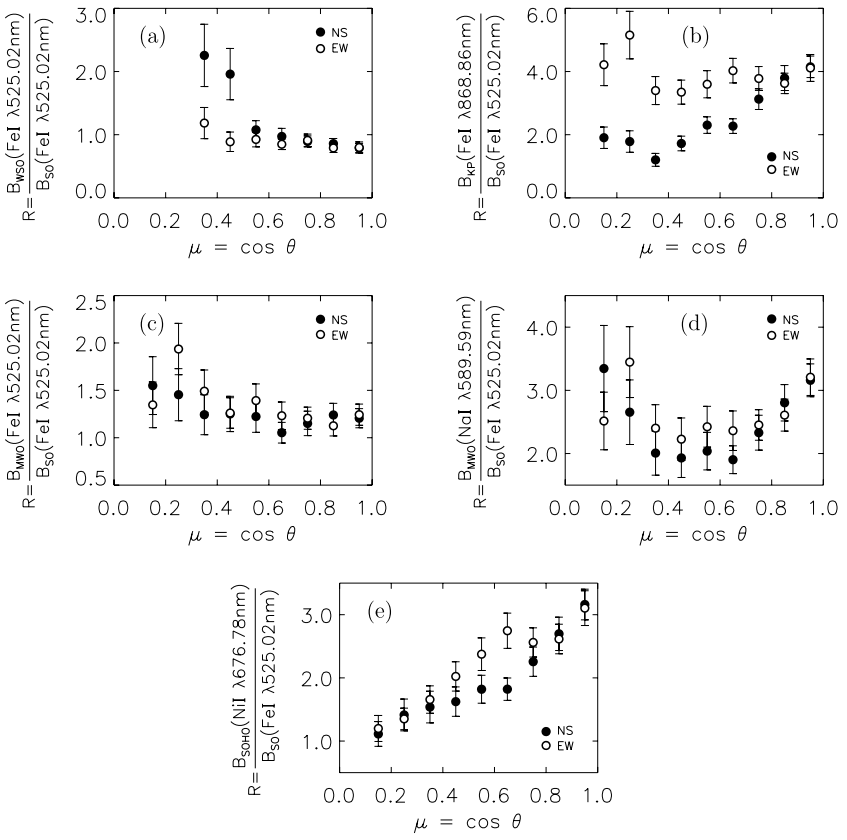

Figure 5 Center-to-limb variations of the strength ratios (regression coefficients R) for the polar (N – S) and equatorial (E – W) sectors of the solar disk obtained for the following combinations of the magnetic field observations: (a) SO – WSO, (b) SO – KP, (c) SO – MWO (Fe I λ525.02 nm), (d) SO – MWO (Na I λ589.59 nm), (e) SO – MDI. The vertical bars at each point are the mean errors of the values.

Going further, in analogy with Figure 5, we calculate distributions of $|B|$ as functions of μ separately for polar and equatorial sectors. The results are presented in Figure 6. A common feature of all plots is the more-or-less smooth behavior from the center to limb (the changes do not exceed by factor of three) of points which belong to the E – W sector, and

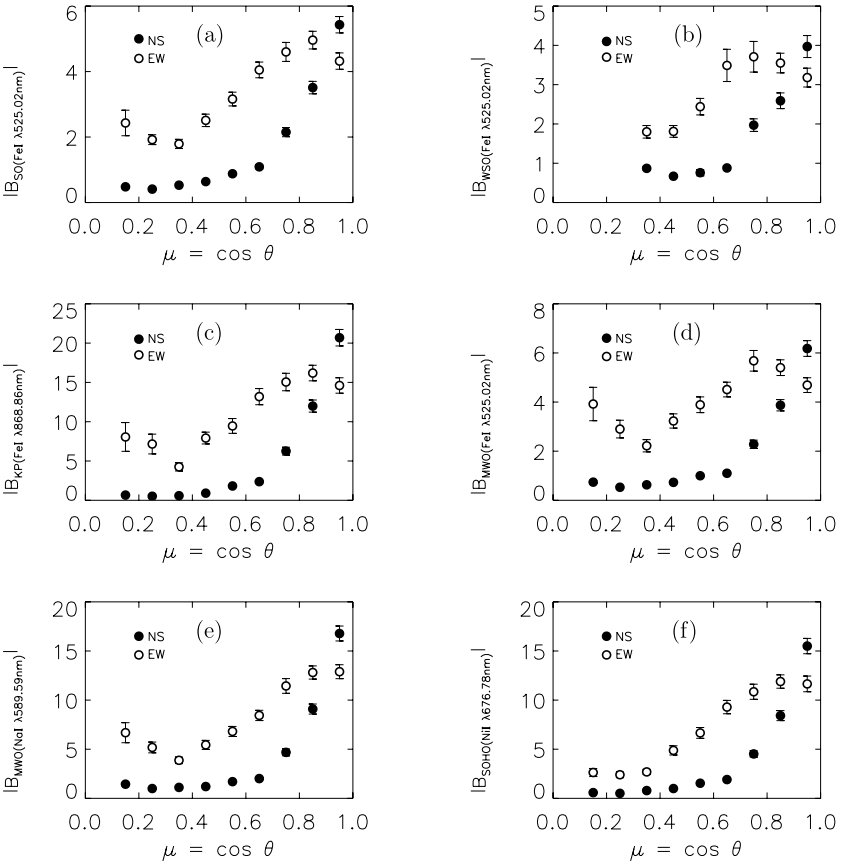

Figure 6 Center-to-limb variations of absolute magnetic strengths $|B|$ for the polar (N – S) and equatorial (E – W) sectors of the solar disk.

sharp decrease for the N – S sector. The mean values of the last three N – S points are 0.47 G for SO, 0.77 G for WSO, 0.58 G for KP, 0.64 G for MWO (Fe I λ525.02 nm), 1.18 G for MWO (Na I λ589.59 nm), and 0.63 G for SoHO. In the extreme case (KP), the decrease of $|B|$ from the central point to the polar limb is about 35 times, for SO this decrease is only equal to 11. One of the important consequences is the impossibility to explain properties of CLV of R for different sectors by properties of CLV of $|B|$. Indeed, significant differences in the CLVs of $|B|$ for different sectors are found for all data sets, but essential differences in R occur only for the combination SO – KP; in the SO – SoHO case they are practically identical. Moreover, according to Figure 2(b) we expected an increase of the KP/SO ratio near the limb where magnetic fields are weaker, but in reality we encounter the opposite situation.

3.2. Comparison of Space *versus* Ground based Data

The next step of the present work is a detailed comparison of solar magnetic fields from SoHO/MDI with ground-based observations at the WSO, KP, and MWO observatories. The original data sets were used in the same way as in the previous section. The results of the

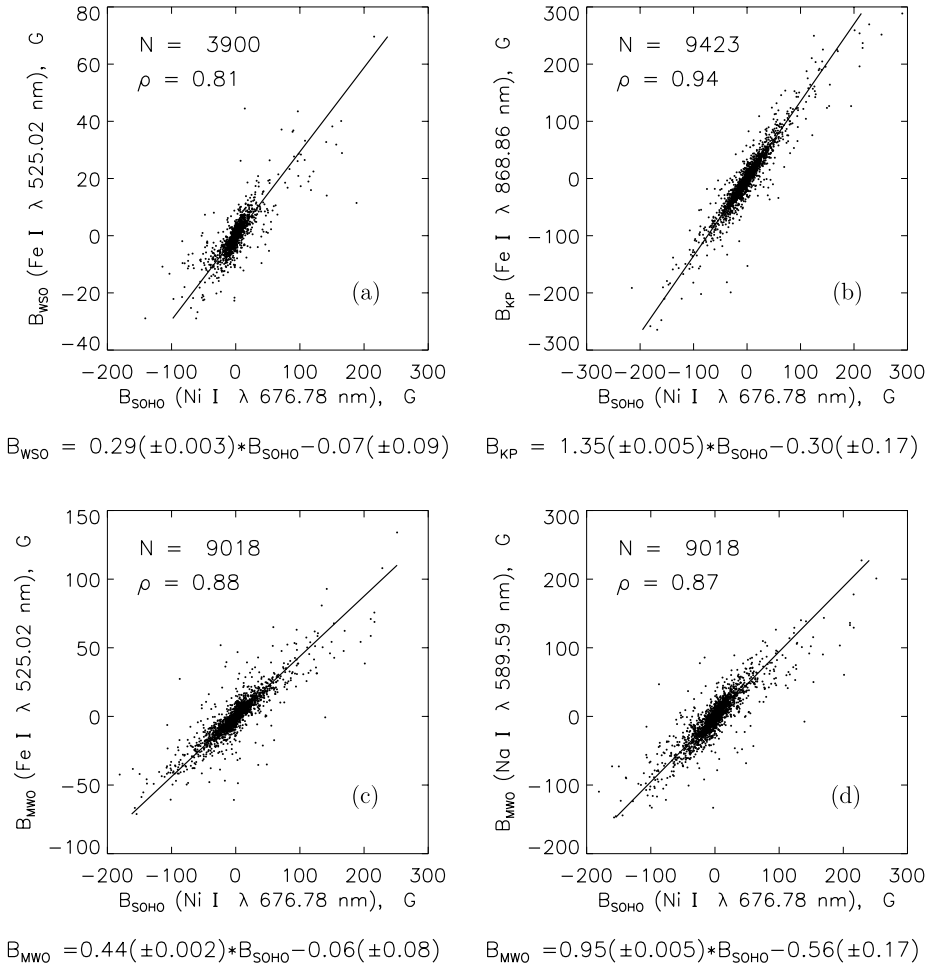

Figure 7 Correlation and regression analysis for different combinations of data sets (a) MDI – WSO, (b) MDI – KP, (c) MDI – MWO (Fe I λ525.02 nm), (d) MDI – MWO (Na I λ589.59 nm). N is the number of common points and ρ the correlation coefficient. The linear regression equations are shown at the bottom of each scatter plot.

analysis are presented basically in the same manner as before. Scatter plots, dependence of R on $|B|$, mosaic maps, CLVs of R for polar and equatorial sectors are presented in Figures 7, 9, 10, and 11.

According to Figure 7, the highest correlation occurs between MDI and KP data (the correlation coefficient is 0.94), but the regression coefficient in this case is equal to 1.35. A good agreement can be seen between the MDI and the MWO (Na I λ589.59 nm) data as well. The correlation coefficient for this combination is 0.87, but the regression coefficient is equal to unity ($R = 0.95$). In the MDI – WSO and MDI – MWO (Fe I λ525.02 nm) cases, the discrepancies are rather strong. The corresponding regression coefficients are equal to 0.29 and 0.44.

To study the dependence of R on $|B|$ in new combinations of data, the corresponding calculations are performed and presented in Figure 9. Again, as in the case of Figure 2, we

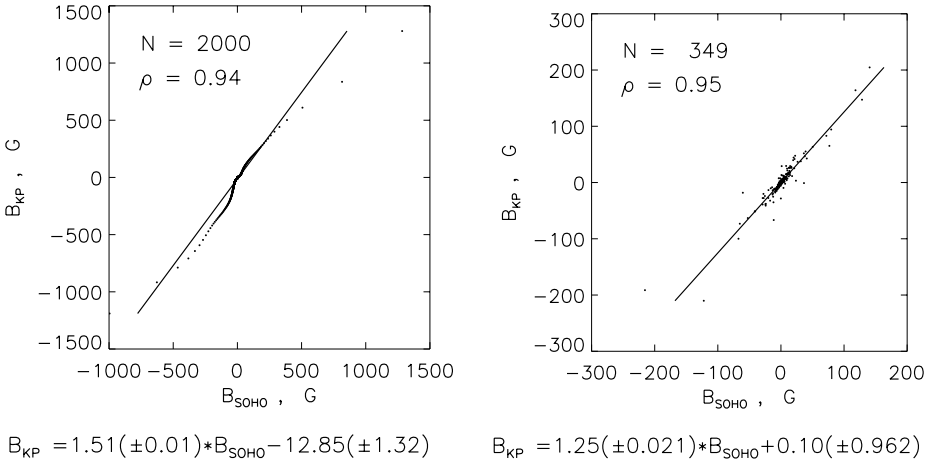

Figure 8 Results of correlation and regression analysis for KP and SoHO/MDI magnetograms. Date of observations is 12 November 2001. Left panel: original spatial resolution and histogram equating method. Right panel: averaging to the SO spatial resolution and pixel-by-pixel comparison.

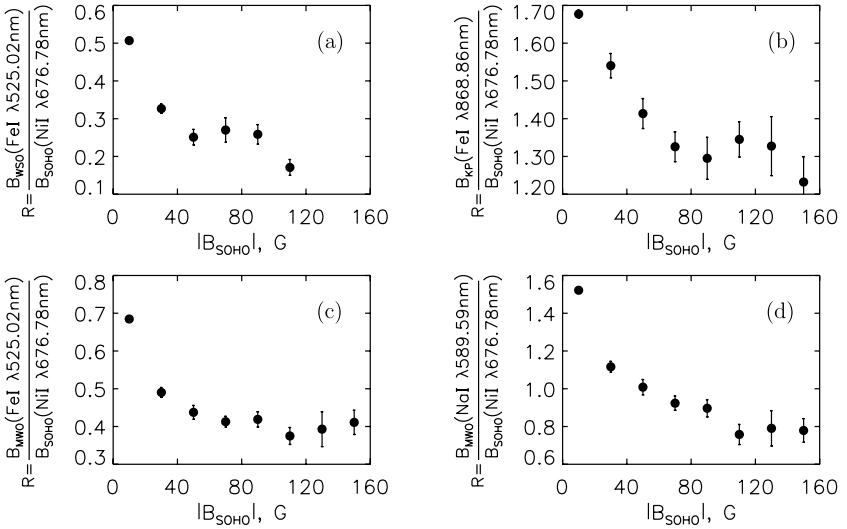

Figure 9 Dependence of the line ratios, considered in Figure 7, on SoHO/MDI magnetic field strength.

see ratios decreasing with increasing magnetic flux. The first bin with an average strength of 10 G in each combination contains the dominant number of points: (a) 3624 among 3900, (b) 8659 among 9423, (c) and (d) 8272 among 9018. In spite of very weak fields in the first bins and possible influence of the noise, their reliability is high (the maximum correlation coefficient is 0.81 for MDI – KP combination and the minimum one is 0.70 for MDI – WSO).

The results from the comparison of KP and SoHO deserve special attention. From previous investigations (Jones and Ceja, 2001; Thornton and Jones, 2002; Wenzler *et al.*, 2004) it is known that field strengths from KP are about 40% weaker than those from SoHO. Almost the same factor of 1.4 is needed, as indicated by Jones and Ceja (2001), to adjust the new

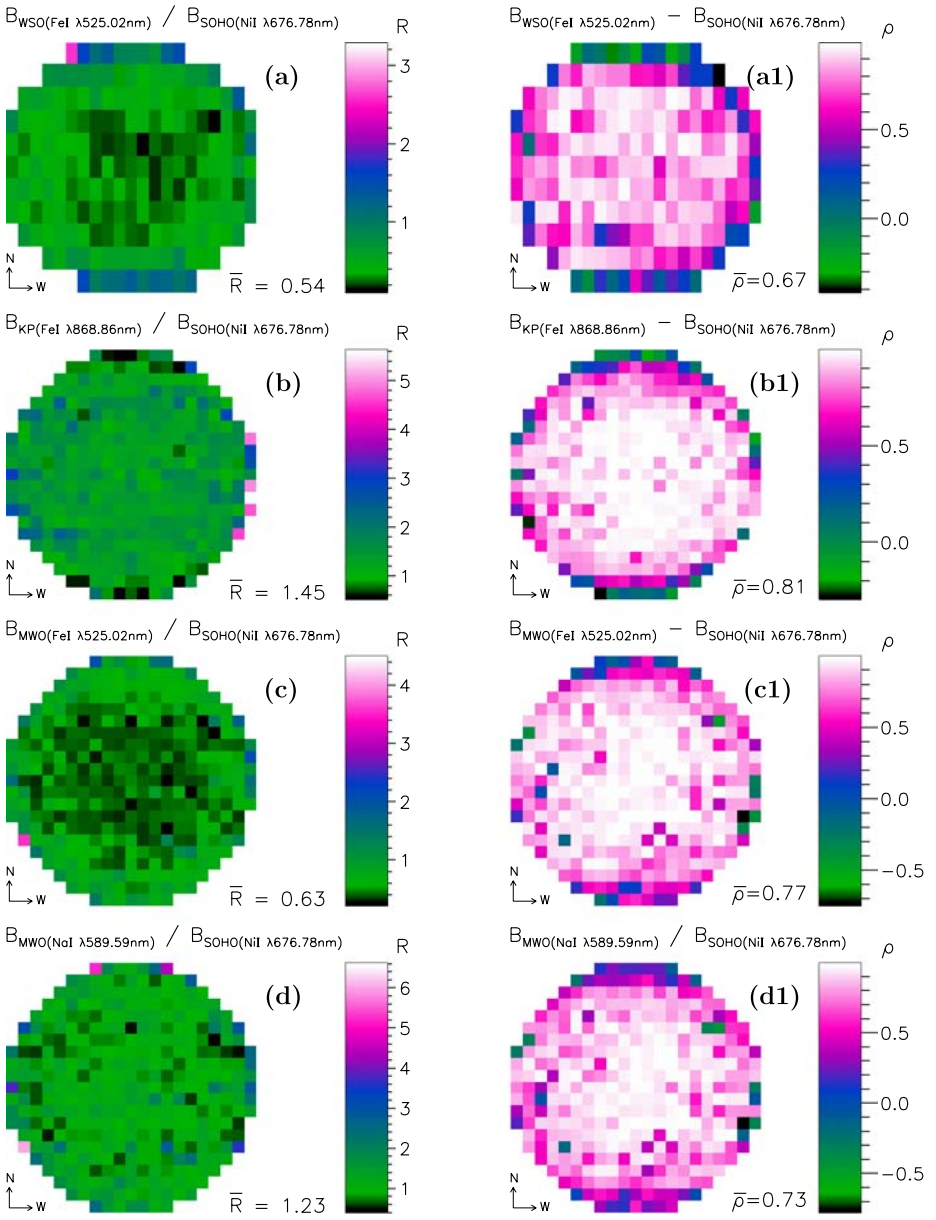

Figure 10 2D distributions of regression (left panels, (a)–(d)) and correlation (right panels, (a1)–(d1)) coefficients across the solar disk for the different combinations of data sets: (a) WSO–MDI, (b) KP–MDI, (c) MWO (Fe I λ525.02 nm)–MDI, (d) MWO (Na I λ589.59 nm)–MDI.

(spectromagnetographical) KP measurements to the old (512-channel Diode Array Magnetograph) ones. At the same time, according to Jones and Ceja (2001), there are almost no systematic differences between KP and GONG$^+$ measurements.

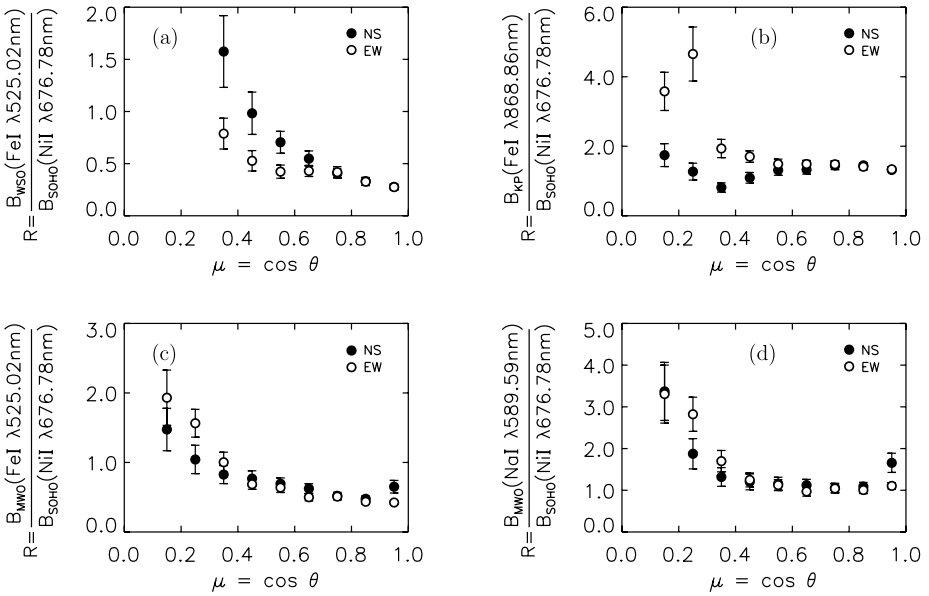

Figure 11 Center-to-limb variations of the strength ratios (regression coefficients R) for the polar (N – S) and equatorial (E – W) sectors of the solar disk obtained for the following combinations of the magnetic field observations: (a) MDI – WSO, (b) MDI – KP, (c) MDI – MWO (Fe I λ525.02 nm), (d) MDI – MWO (Na I λ589.59 nm).

In our study we have already applied the factor of 1.46 to the KP data according to Harvey's recommendation, as mentioned before. If we had the same correspondence between KP and SoHO, as in above cited studies, we should have the ratio KP – SoHO close to unity but this is not the case. However, our main goal is to explore the spatial distributions of R across the solar disk in different combinations of data sets, and therefore it is beyond the frames of this paper to clarify this discrepancy. Nevertheless it is worth to be investigated in more details in a separate work.

Naturally the idea arises that the difference could be explained by the difference in time of the observations: May – June 2000 in (Jones and Ceja, 2001) and April – December 2001 in our study. But both periods of time belong to a similar level of solar activity, and Wenzler *et al.* (2004), using 24 days between 1997 and 2001, obtained SoHO – KP slope almost identical to that obtained by Jones and Ceja (2001). Therefore, the time difference can hardly play a decisive role in this problem (although it deserves of careful considerations in other issues). An independent support of this statement comes from the analysis of long-term observations of the Sun-as-a-star magnetic field at SO. We have investigated the line ratios for different combinations of four lines near Fe I λ525.02 nm for the period from 1999 to 2006 and we do not find significant time variations correlated to the solar activity cycle, in agreement with already published results (Demidov *et al.*, 2002) for the period 1999 – 2001. We have also performed a comparison of regression coefficients for MWO – SoHO and MWO(Na I λ589.59) – MWO(Fe I λ525.02) combinations for the extreme cases of maximum (26 days of observations in 2001) and minimum (25 days of observations in March 2007) of solar activity. For the combination MWO(Na I λ589.59) – SoHO we obtain $R = 0.95$ for 2001, and $R = 1.28$ for 2007. For the combination MWO(Fe I λ525.02) – SoHO $R = 0.44$ and $R = 0.51$ are found, and for the combination MWO(Na I λ589.59) – MWO(Fe I λ525.02)

$R = 2.16$ and $R = 2.50$. For all cases the correlation coefficients are large, and the minimum one is equal to 0.88 for MWO(Fe I λ525.02) – SoHO, 2001.

Other reasons for the discrepancy between our and previous results could be the use of data with different spatial resolution and different methods for the analysis. We average the data to the spatial resolution of SO and use the pixel-by-pixel (PbP) comparison, while all three groups of authors mentioned above use the original KP and MDI spatial resolution and the histogram-equating (HE) method. To find out which reason (or both) is responsible for the discrepancy, we perform the additional investigation described in the following.

Obviously, in the presence of non-linearity in the relationship between data sets for different magnetic field strengths, spatial averaging of weak and strong magnetic fields will lead to changes (which certainly depend on the degree of non-linearity) of the regression coefficients even if we use the same method of analysis. Of course, the use of different methods can affect the results as well.

In the first step, in order to exclude the influence of different spatial resolution on the results, we calculate the regression KP – SoHO coefficients using HE method and original KP and MDI resolutions for several days. For the HE calculations we use the approach described by Wenzler *et al.* (2004). We obtain the following numbers: 8 November 2001, $R = 1.84(\pm 0.01)$; 12 November 2001, $R = 1.51(\pm 0.01)$; 16 November 2001, $R = 1.76(\pm 0.01)$; 21 November 2001, $R = 2.10(\pm 0.01)$. The result for 12 November 2001 is presented in Figure 8 (left panel). Because in these calculations we use the same magnetograms as in our previous analysis, the time of the SoHO observations coincides with the observations at SO and, consequently, differ (on about 12 hours) from the KP time. But it hardly ever plays a significant role: calculations for simultaneous KP and MDI magnetograms for 12 November 2001 give $R = 1.75(\pm 0.01)$.

In the second step, to evaluate the influence of spatial resolution, calculations for data averaged to the SO aperture are made using both PbP and HE methods. The corresponding scatter plot for 12 November 2001 is shown in the right panel of Figure 12. In this case we obtain $R = 1.25(\pm 0.02)$. The HE method gives $R = 1.32(\pm 0.02)$ for such data, what is very close to the previous estimation.

Several conclusions are obtained from the consideration of Figure 8 and the results mentioned above. Firstly, the use of the HE method for the data with high spatial resolution gives different results, the discrepancy between us and other authors increases even more than using the PbP method. Secondly, there is a difference between results obtained by the PbP method for data with low spatial resolution and by the HE method for the data with high spatial resolution. Thirdly, there is no significant difference between PbP and HE results for data with low spatial resolution.

Most probably, from our point of view, the common reason for all these results is the big non-linearity in the relationship between KP and MDI data, and, as a consequence, a very complicated character of the HE curves. As it will be shown in the next section, when data relations are more linear, the difference between PbP and HE methods is rather small. But from the left panel of the Figure 8 it is easy to see that the distribution of points near the $B \approx 0$ (the number of such points is overpowering) and for strong fields is quite different: $R = (2.19 \pm 0.02)$ for $|B| \leq 100$ G, and $R = (1.05 \pm 0.01)$ for $B \geq 50$ G and $R = (1.23 \pm 0.03)$ for $B \leq -50$ G. Even more, the results depend on polarity. For other days, the situation is the same or even worse. If we exclude points with weak field strength from the HE analysis, the agreement with PbP results is much better. The cause to exclude weak fields from HE analysis follows from simple circumstances: with noisy, non-correlated data, the PbP method gives zero correlation and an undetermined regression, while the HE method gives wrong perfect correlations and significant regressions.

Using spatial averaging, we decrease the range of strengths and, being more important, the non-linearity of the data sets. As a consequence, we have a good correspondence of HE and PbP methods. If we assume that the authors of the mentioned papers use some preliminary selection of data and we restrict our calculations by some limitations, we can reach an agreement of our HE results. Indeed, for $B \geq 100$ G we have $R = 0.99(\pm 0.01)$, and for $B \leq -100$ G, we have $R = 1.12(\pm 0.04)$, on average $R = 1.05$, which, taking into account the correction coefficient of 1.46 for KP, practically coincides with the values obtained by other authors. There are some indications that some kind of filtration of the data was really used by those authors. In the paper of Wenzler *et al.* (2004) we read: "... there is considerable scatter from one day to the other so that the exact choice of dates is relevant. Details such as the limiting values ($\mu = \cos\theta$, where θ is the heliocentric angle) also play a role, especially since MDI data suffer from very strong noise at some locations right at the limb". Maybe as a result of such selections, we have a range of strengths of ± 1500 G in our full disk case, while their range of strengths does not exceed 800 G.

Figure 10 presents the corresponding mosaic distributions of the linear regression coefficients across the solar disk. Comparing the MDI data with the observations performed in the line Fe I λ525.02 nm (WSO and MWO), we see similar patterns. In the MDI–KP case, the results for the central part of the disk do not reveal an appreciable CLV. However, there is a remarkable difference between the polar and equatorial areas near the limb. The comparatively high R values for some points on the W-limb in this case are most likely an artifact, caused by the compensation of the solar rotation (in 25 cases out of 27 the KP magnetograms were obtained by rotation from west to east). For the combination MDI – MWO (Na I λ589.59 nm) the behavior of the regression coefficients in polar and equatorial directions is practically the same, being almost constant at the central part of the disk and increasing near the limb.

The main conclusions from the analysis of Figure 10 are supported by the more detailed study of the CLV of the R coefficients as presented in Figure 11. Indeed, for the MDI – WSO and MDI – MWO (Fe I λ525.02 nm) combinations, almost identical $R(\mu)$ curves for both sectors are found, except for some differences at the polar regions of the N – S sector. For the MDI – KP case, $R(\mu)$ remains close to 1.5 over almost the whole disk. The relatively high R values at the E-W sector with $\mu = 0.2 - 0.3$ and $\mu = 0.1 - 0.2$ are of artificial nature. Comparing the MDI with the MWO (Na I λ589.59 nm) data, we see that R is close to 1 within 60° from the disk center ($\mu > 0.5$). With further increase of the heliocentric distance, the regression coefficients change rather quickly up to 3.5, practically synchronously in the N – S and E – W sectors.

At the end of this section it is worth noting that the results of our calculations for the MWO (Fe I λ525.029 nm) – MDI combination are confirmed by Tran *et al.* (2005). Indeed, according to our Figure 11, we have $R = 0.40$ for the disk center. But we obtain 1.8 when we use MWO measurements after applying the correction function (CF) suggested by Tran *et al.* (2005) for the Fe I λ525.029 nm line (for the disk center CF = 4.5). This number practically coincides with the results of Tran *et al.* (2005) given in their Table 3 and Figure 6. Our full-disk calculations for one of the days (31 March 2001) yield $R = 0.41(\pm 0.01)$ for the non-corrected data, and $R = 1.57(\pm 0.05)$ for the corrected data. Clearly, this result is very close to the disk average coefficient of 1.7 found by Tran *et al.* (2005).

3.3. Comparison of MWO Magnetograms in Two Spectral Lines and SO Magnetograms in Four Spectral Lines

Figure 12 (left panel) presents a scatter plot of magnetic field strengths measured at MWO in the spectral lines Fe I λ525.02 and Na I λ589.59 nm. The regression coefficient in this

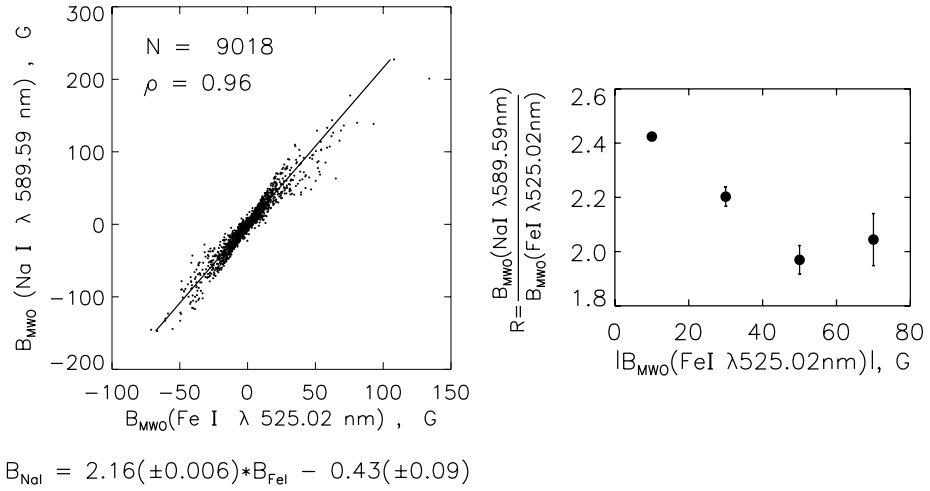

Figure 12 Left panel: results of correlation and regression analysis for MWO magnetograms obtained in the Fe I λ525.02 nm and Na I λ589.59 nm spectral lines. Right panel: dependence of R ratios for the data from left panel on the magnetic field strength in Fe I λ525.02 line.

case is equal to 2.15 with a quite high correlation coefficient, $\rho = 0.96$. The results of the calculations of R for different magnetic field strengths (dependence of R on $|B|$) are shown in the right panel of Figure 12.

Figure 13 shows the spatial distribution of the coefficients R and ρ across the solar disk. Figure 14 shows CLV of R for the polar and equatorial sectors. Significant CLVs of the R coefficients are practically identical for the NS and EW sectors. With decreasing μ from 1.0 to 0.5, the R values decrease approximately from 2.6 to 1.7 and then again rise to 2.

Simultaneous observations at MWO in different spectral lines allow to test the influence of the spatial averaging on the regression analysis. Observations made on 31 March 2001 were used for this purpose. With the original MWO spatial resolution (the number of points 202195, the correlation coefficient $\rho = 0.95$, for the range of B ±500 G), the following equation was obtained: $B_{\mathrm{Na\,I}\lambda589.59} = (0.07 \pm 0.052) + (1.89 \pm 0.001) \times B_{\mathrm{Fe\,I}\lambda525.02}$. After averaging the observations to the spatial resolution of SO (see Section 3.1), the results change a little: $B_{\mathrm{Na\,I}\lambda589.59} = (0.07 \pm 0.542) + (2.18 \pm 0.028) \times B_{\mathrm{Fe\,I}\lambda525.02}$. The number of points in this case is 349, $\rho = 0.97$, and the range of B is within ±60 G. The 15% increase of R is most probably caused by the non-linearity of the regression: R is less for big strengths than for small strengths.

After applying the histogram-equating method to these original MWO observations, we obtain $R = 1.98$ for the magnetic flux distributed over 200 bins, and $R = 2.06$ distributing the flux over 50 bins. We see that the different methods of regression analysis give different results. This seems to be unavoidable in the presence of a dispersion of points and a deflection from linearity.

In general, quasi-simultaneous observations of the Sun-as-a-star and large-scale magnetic fields are available at SO in several spectral lines (Demidov *et al.*, 2002), usually in four lines: Fe I λ524.70 nm ($g = 2$), Cr I λ524.76 nm ($g = 2.5$), Fe I λ525.02 nm ($g = 3.0$), and Fe I λ525.06 nm ($g = 1.5$). The results of calculations of CLV for all possible MSR combinations are presented in Figure 15. The CLV of MSR in some combinations of spectral lines (524.75 – 524.70; 525.06 – 524.70; 525.02 – 524.75) in polar and equatorial sectors are almost indistinguishable (especially in the last case), but they are very well pronounced in

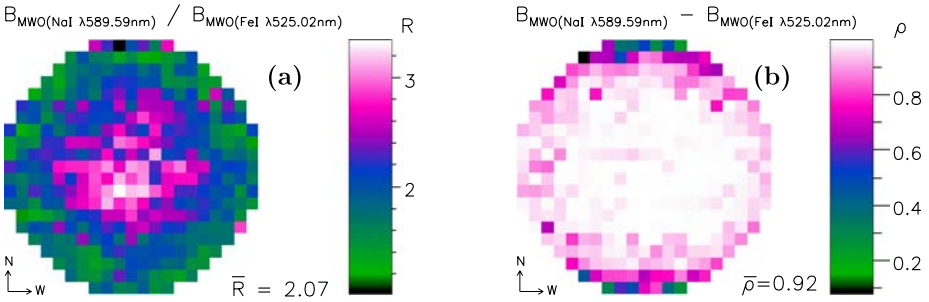

Figure 13 2D distributions of (a) regression and (b) correlation coefficients across the solar disk for MWO magnetograms obtained in the Fe I λ525.02 and Na I λ589.59 spectral lines.

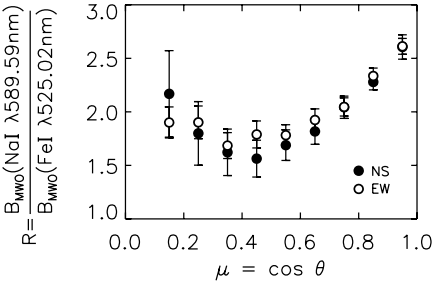

Figure 14 Center-to-limb variations of the strength ratios (regression coefficients R) for the "polar" (N – S) and "equatorial" (E – W) sectors of the solar disk obtained for MWO magnetograms in the Fe I λ525.02 nm and Na I λ589.59 nm spectral lines.

the three other combinations, particularly in the 525.06 – 525.02 case. Such variations of the CLV of MSR could mean that the effect of polar – equator asymmetries is most likely connected with peculiarities of the polarized radiation transfer in different spectral lines.

4. Discussion and Conclusion

The results presented in the previous sections provide a new experimental basis for solar physics activities related to magnetic field measurements and interpretations. They have demonstrated that quasi-simultaneous magnetic field observations exhibit a rather high level of correlation, in spite of their measurement with different instruments and in different spectral lines. In general, it proves the high reliability of data sets from different observatories, at least of those used in the present investigation. This statement is corroborated by $R \approx 1$ in those cases, when observations at different observatories in the same spectral line (here in Fe I λ525.02 nm) are compared. Sometimes $R \approx 1$ is observed even in data sets obtained in different spectral lines: MDI (Ni I λ676.78 nm) – KP (Fe I λ868.86 nm) and MDI (Ni I λ676.78 nm) – MWO (Na I λ589.59 nm). From Table 2 we see that low level excitation potentials and Landé factors of the compared lines are quite close to each other in the first case; but in the second case the excitation potentials differ strongly. From the analysis of

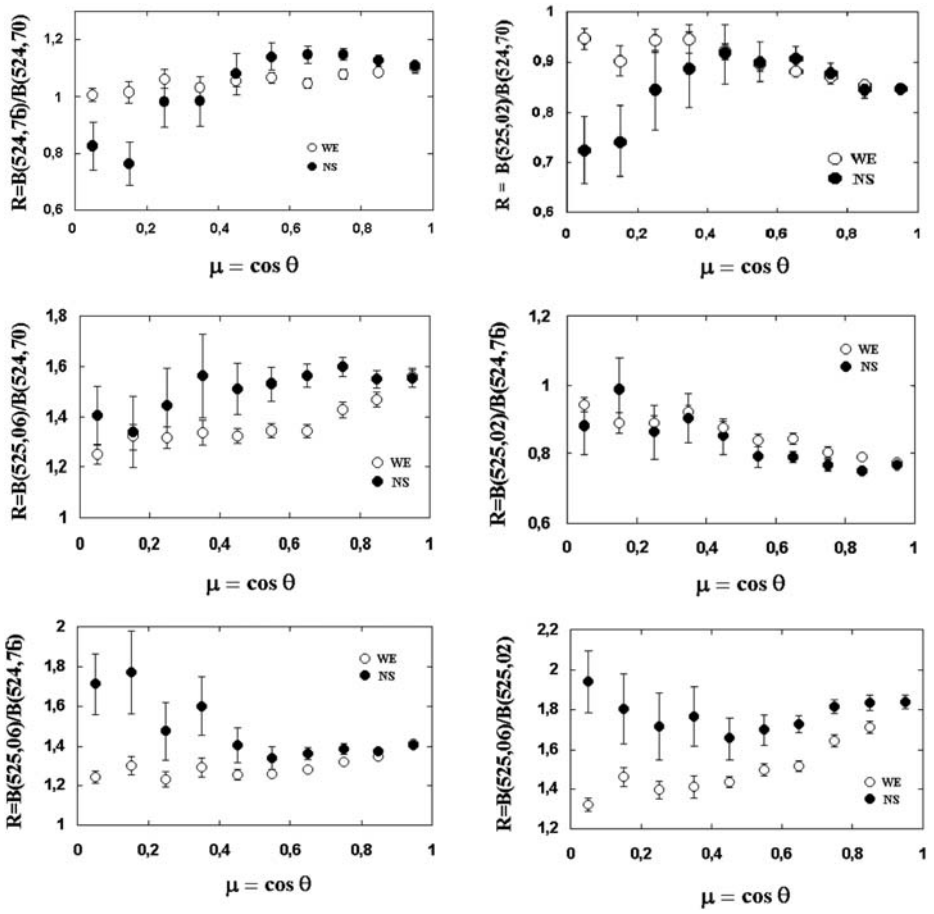

Figure 15 Center-to-limb variations of the strength ratios (regression coefficients R) for the polar (N – S) and equatorial (E – W) sectors of the solar disk obtained for all possible combinations of four spectral lines in the vicinity of Fe I λ525.02 nm. 35 full-disk magnetograms observed from 01 April 2001 to 01 February 2002 at the Sayan observatory are used.

Figures 1(c) and 12 (left panel) it is evident that in the first case (SO (Fe I λ525.02 nm) – MWO (Na I λ589.59 nm), $\rho = 0.83$) the scatter of the points is larger than in the second case (MWO (Fe I λ525.02 nm) – MWO (Na I λ589.59 nm), $\rho = 0.96$). The regression coefficients for both data sets are very close to each other (2.53 and 2.15, respectively). The smaller ρ in the first combination can be explained by instrumental differences, the difference in time, observation conditions, and so on.

Concerning the systematic differences (by factors of 2 – 4 in our cases) between observations in different spectral lines (at the same telescope or at different observatories), this information points at a great physical challenge. It becomes especially evident that there are some tendencies of a dependence of the results on wavelength and Landé factor g. Indeed, if we consider MSR relative to the Fe I λ525.02 nm, an almost linear dependence on wavelength exists. And there is a tendency of increasing MSR with decreasing g. The first attempt to reproduce this effect by numerical calculations of line properties using the DMG-code by Grossmann-Doerth, Larsson, and Solanki (1988) did not support the increase with wave-

length. The calculation of artificial spectral lines, where all parameters, except (1) wavelength or (2) g-factor, are constant, have shown a decrease of MSR with wavelength and g. But certainly, the amount of data is not large enough to arrive at a final conclusion. More studies in this respect are necessary. A more detailed consideration of such phenomena is a very extensive issue beyond the goals of the present paper, and it will be the subject of a special investigation in the future. The same is valid for the discovered existence of great inhomogeneities in the spatial distribution of the regression coefficients across the disk of the Sun.

The first idea arising from the different CLVs of R for different combinations of spectral lines is a possible influence of variations of spectral line profiles across the solar disk. Indeed, the parameters of the majority of Fraunhofer line profiles show CLVs, the nature of which are mainly determined by the formation heights of the lines (Gopasyuk *et al.*, 1973; Balthasar, 1984). In particular, Balthasar (1984) has shown that in the solar disk center ($0.8 < \mu < 1.0$) almost all lines have a C shape and a blue asymmetry. But close to the limb, many spectral lines show a different type of asymmetry. This allows to subdivide the spectral lines into three classes: those with an increase of the blue asymmetry, with a change to a red asymmetry, and those retaining the original C shape. The commonly used Fe I λ525.02 nm line is assigned by the author to the latter class, *i.e.*, the form of this line shows insignificant center-to-limb variations.

However, these phenomena did not have any great significance for the magnetic field strength analyses, because existing information about the spectral line profile parameters are taken into account automatically in the process of calibration. Most likely, the only chance for a quantitative interpretation of the magnetic strength ratio variations lies in modeling the polarized radiative transfer through the complex, spatially structured, dynamic medium. First attempts with some simplified assumptions were made by Solanki *et al.* (1998) and by Demidov, Veretsky, and Peshcherov (2003). The results of these two papers for the CLV of the $B(525.02)/B(524.70)$ ratio are rather similar to each other. Namely, there is a rather good agreement of experimental and theoretical values for the central part of the solar disk, but with increasing distance from the center, discrepancies appear. In particular, the theory predicts a change of the R ratio from a value < 1.0 values to one > 1.0 at $\mu = 0.6(\pm 0.1)$, depending on the model parameters. But according to observations this value remains <1.0 for all μ. The reasons for such discrepancies remain unclear yet, and there is a need for further investigations.

Detailed, complex, and rather realistic 3D simulations of magnetic convection in the solar photosphere and convective zone are now available (see, *e.g.*, Vögler *et al.*, 2005; Stein and Nordlund, 2006). They include variations of all physical parameters on very different temporal and spatial scales down to scales which cannot be resolved by present observations. For a snapshot of the simulations such theoretical data have already been used to calculate Stokes profiles of mixed polarity regions (*e.g.*, Khomenko *et al.*, 2005; Khomenko and Collados, 2007). Carroll and Staude (2003; 2005) and Carroll and Kopf (2007) have developed a stochastic formulation of polarized radiative transfer valid for arbitrary correlation lengths of the spatial fluctuations of the physical parameters, producing the Stokes parameters as the macroscopic observables (expectation values). The magnetic convection simulations can provide the probability distribution functions of the physical parameters (magnetic field, velocity, temperature, *etc.*) by means of which the stochastic polarized radiative transfer code can calculate the observable Stokes parameters. These, in its turn, can be used in a Stokes profile inversion code (*e.g.*, Carroll and Staude, 2001) to provide a more reliable base for a comparison of the observations described in the present paper with the theoretical predictions.

Acknowledgements We are thankful to R.M. Veretsky, V.S. Pescherov, T.A. Latushko, and G.S. Vasiljeva for assistance in obtaining and processing the observation material at the STOP telescope of the Sayan Observatory. The authors are also grateful to J. Sommers, T. Hoeksema (Wilcox Solar Observatory), and to J. Harvey (Kitt Peak National Observatory) for advice concerning the problems of solar magnetic field observations at the corresponding observatories. We express our gratitude to T. Hoeksema and J. Sommers for the data (of the first level) from the Wilcox Solar Observatory. The authors thank V.V. Grechnev (ISTP) sincerely for important suggestions on the IDL use and C. Denker and T. Carroll (AIP) for useful comments and remarks.

The authors are in debt to the anonymous referee for comments and suggestions that helped to improve this paper.

This study includes data from the synoptic program at the 150-Foot Solar Tower of the Mt. Wilson Observatory. The Mt. Wilson 150-Foot Solar Tower is operated by UCLA, with funding from NASA, ONR and NSF, under agreement with the Mt. Wilson Institute.

NSO/Kitt Peak data used here are produced cooperatively by NSF/NOAO, NASA/GSFC, and NOAA/SEL.

The MDI data from the SoHO spacecraft used in this study are produced by the Stanford-Lockheed Institute for Space Research and the Solar Oscillations Investigation (SOI) in the W.W. Hansen Experimental Physics Laboratory of Stanford University and the Solar and Astrophysics Laboratory of the Lockheed-Martin Advanced Technology Center, USA. We took the magnetograms from the web-site http://soi.stanford.edu/data/ supported by the SOI and MDI team.

The results presented in this study were obtained partly due to support by the RFBR grant 05-02-16472 and by the DFG (German Science Foundation) grants 436 RUS 113/784/0-1 and BA 1875/4-1.

References

Arge, C.N.: 2004, In: AGU Fall Meeting, SH52A-02.
Arge, C.N., Hildner, E., Pizzo, V.J., Harvey, J.W.: 2002, *J. Geophys. Res.* **107**(A10), SSH 16-1.
Balthasar, H.: 1984, *Solar Phys.* **93**, 219.
Berger, T.E., Lites, B.W.: 2003, *Solar Phys.* **213**, 213.
Bruls, J.H.M.J., Lites, B.W., Murphy, G.A.: 1991, In: November, L.J. (ed.) *Solar Polarimetry*, National Solar Observatory, Sacramento Peak, 444.
Carroll, T.A., Kopf, M.: 2007, *Astron. Astrophys.* **468**, 323.
Carroll, T.A., Staude, J.: 2001, *Astron. Astrophys.* **378**, 316.
Carroll, T.A., Staude, J.: 2003, In: Trujillo Bueno, J., Sánchez Almeida, J. (eds.) *Solar Polarization 3, ASP Conf. Ser.* **307**, 125.
Carroll, T.A., Staude, J.: 2005, *Astron. Nachr.* **326**, 296.
Chaplin, W.J., Dumbill, A.M., Elsworth, Y., Isaak, G.R., McLeod, C.P., Miller, B.A., New, R., Pinter, B.: 2003, *Mon. Not. Roy. Astron. Soc.* **343**, 813.
Davis, J.C.: 1986, *Statistics and Data Analysis in Geology*, Wiley, New York, 636.
Demidov, M.L.: 2000, *J. Astrophys. Astron.* **21**, 209.
Demidov, M.L., Golubeva, E.M.: 2004, In: Stepanov, A.V., Benevolenskaya, E.E., Kosovichev, A.G. (eds.) *Multiwavelength Investigations of Solar Activity, IAU Symp.* **223**, 211.
Demidov, M.L., Veretsky, R.M., Peshcherov, V.S.: 2003, In: Trujillo Bueno, J., Sánchez Almeida, J. (eds.) *Solar Polarization 3, ASP Conf. Ser.* **307**, 352.
Demidov, M.L., Zhigalov, V.V., Peshcherov, V.S., Grigoryev, V.M.: 2002, *Solar Phys.* **209**, 217.
Domínguez Cerdeña, I., Sánchez Almeida, J., Kneer, F.: 2003, *Astron. Astrophys.* **407**, 741.
Frazier, E.N., Stenflo, J.O.: 1972, *Solar Phys.* **27**, 330.
Gopasyuk, S.I., Kotov, V.A., Severny, A.B., Tsap, T.T.: 1973, *Solar Phys.* **31**, 307.
Grossmann-Doerth, U., Larsson, B., Solanki, S.K.: 1988, *Astron. Astrophys.* **204**, 266.
Hofmann, A., Grigorjev, V.M., Selivanov, V.L., Ivana, M.: 1988, *Astron. Nachr.* **309**, 331.
Howard, R., Harvey, J.W.: 1970, *Solar Phys.* **12**, 23.
Howard, R., Stenflo, J.O.: 1972, *Solar Phys.* **22**, 402.
Jones, H.P., Ceja, J.A.: 2001, In: Sigwarth, M. (ed.) *Advanced Solar Polarimetry – Theory, Observation, and Instrumentation, ASP Conf. Ser.* **236**, 87.
Khomenko, E., Collados, M.: 2007, *Astrophys. J.* **659**, 1726.
Khomenko, E.V., Shelyak, S., Solanki, S.K., Vögler, A.: 2005, *Astron. Astrophys.* **442**, 1059.
Kotov, V.A.: 2002, *Astron. Astrophys.* **402**, 1145.
Kotov, V.A., Kotov, S.V., Setyev, V.V.: 2002, *Solar Phys.* **209**, 233.
Lockwood, M., Stamper, R., Wild, M.N.: 1999, *Nature* **399**, 437.
Norton, A.A., Ulrich, R.K.: 2000, *Solar Phys.* **192**, 403.

Ronan, R.S., Orrall, F.Q., Mickey, D.L., West, E.A., Hagyard, M.J., Balasubramaniam, K.S.: 1992, *Solar Phys.* **138**, 49.
Sánchez Almeida, J., Domínguez Cerdeña, I., Kneer, F.: 2003, *Astrophys. J.* **597**, L177.
Sheminova, V.A.: 1998, *Astron. Astrophys.* **329**, 721.
Shrauner, J.A., Scherrer, P.H.: 1994, *Solar Phys.* **153**, 131.
Semel, M.: 1981, *Astron. Astrophys.* **97**, 75.
Snodgrass, H.B., Kress, J.M., Wilson, P.R.: 2000, *Solar Phys.* **191**, 1.
Socas-Navarro, H., Borrero, J.M., Asensio Ramos, A., Collados, M., Domínquez Cerdeña, I., Khomenko, E.V., Martínez Gonzálas, M.J., Martínez Pillet, V., Ruiz Cobo, B., Sánchez Almeida, J.: 2008, *Astrophys. J.* **674**, 596.
Solanki, S.K., Stenflo, J.O.: 1984, *Astron. Astrophys. Suppl.* **140**, 185.
Solanki, S.K., Stenflo, J.O.: 1985, *Astron. Astrophys. Suppl.* **148**, 123.
Solanki, S.K., Steiner, O., Bünte, M., Murphy, G., Ploner, S.R.O.: 1998, *Astron. Astrophys.* **333**, 721.
Stein, R.F., Nordlund, A.: 2006, *Astrophys. J.* **642**, 1246.
Stenflo, J.O.: 1973, *Solar Phys.* **32**, 41.
Stenflo, J.O., Harvey, J.W.: 1985, *Solar Phys.* **95**, 99.
Stenflo, J.O., Solanki, S.K., Harvey, J.W.: 1987, *Astron. Astrophys.* **171**, 305.
Su, J.T., Zhang, H.Q.: 2007, *Astrophys. J.* **666**, 559.
Svalgaard, L.: 2005, In: AGU Spring Meeting, SH23C-05.
Thornton, C.E., Jones, P.H.: 2002, *Bull. Am. Astron. Soc.* **34**, 1243.
Tran, T., Bertello, L., Ulrich, R.K., Evans, S.: 2005, *Astrophys. J. Suppl.* **156**, 295.
Ulrich, R.K.: 1992, In: Giampapa, M.S., Bookbinder, J.M. (eds.) *Proc. 7th Cambridge Workshop, Cool Stars, Stellar Systems, and the Sun, ASP Conf. Ser.* **26**, 265.
Ulrich, R.K., Evans, S., Boyden, J.E., Webster, L.: 2002, *Astrophys. J. Suppl.* **139**, 259.
Vernazza, J.E., Avrett, E.H., Loeser, R.: 1981, *Astrophys. J. Suppl.* **45**, 635.
Vögler, A., Shelyak, S., Schüssler, M., Cattaneo, F., Emonet, T., Linde, T.: 2005, *Astron. Astrophys.* **429**, 335.
Wang, H., Sheeley, N.R. Jr.: 1995, *Astrophys. J.* **447**, L143.
Wang, H., Varsik, J., Zirin, H., Canfield, R.C., Leka, K.D., Wang, J.: 1992, *Solar Phys.* **142**, 11.
Wenzler, T., Solanki, S.K., Krivova, N.A.: 2005, *Astron. Astrophys.* **432**, 1057.
Wenzler, T., Solanki, S.K., Krivova, N.A., Fluri, D.M.: 2004, *Astron. Astrophys.* **427**, 1031.
Wiehr, E.: 1978, *Astron. Astrophys.* **69**, 279.
Zayer, I., Solanki, S.K., Stenflo, J.O., Keller, C.U.: 1990, *Astron. Astrophys.* **239**, 356.
Zhang, H., LaBonte, B., Li, J., Sakurai, T.: 2003, *Solar Phys.* **213**, 87.